Nuclear Electroweak Densities and Moments in Nuclear DFT

Witold Nazarewicz, FRIB@MSU

Mean-field and Cluster Dynamics in Nuclear Systems (MCD 2022)

YITP Kyoto June 9, 2022

In collaboration with P.-G. Reinhard, X. Roca—Maza, …

This presentation complements J. Dobaczewski's talk on DFT description of nuclear electromagnetic moments

Menu

- Nuclear charge densities and charge radii
- Mirror radii differences
- Searches for BSM physics
- Parity-violating asymmetry measured by PREX-2 and CREX
- Perspectives

Guiding principle: the scientific method…

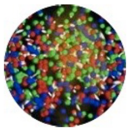

Hot and Dense Nuclear Matter

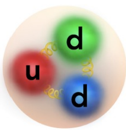

Hadrons

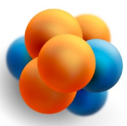

Atomic Nucleus

Nuceli in the Cosmos

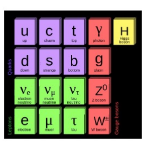

Fundamental Interactions

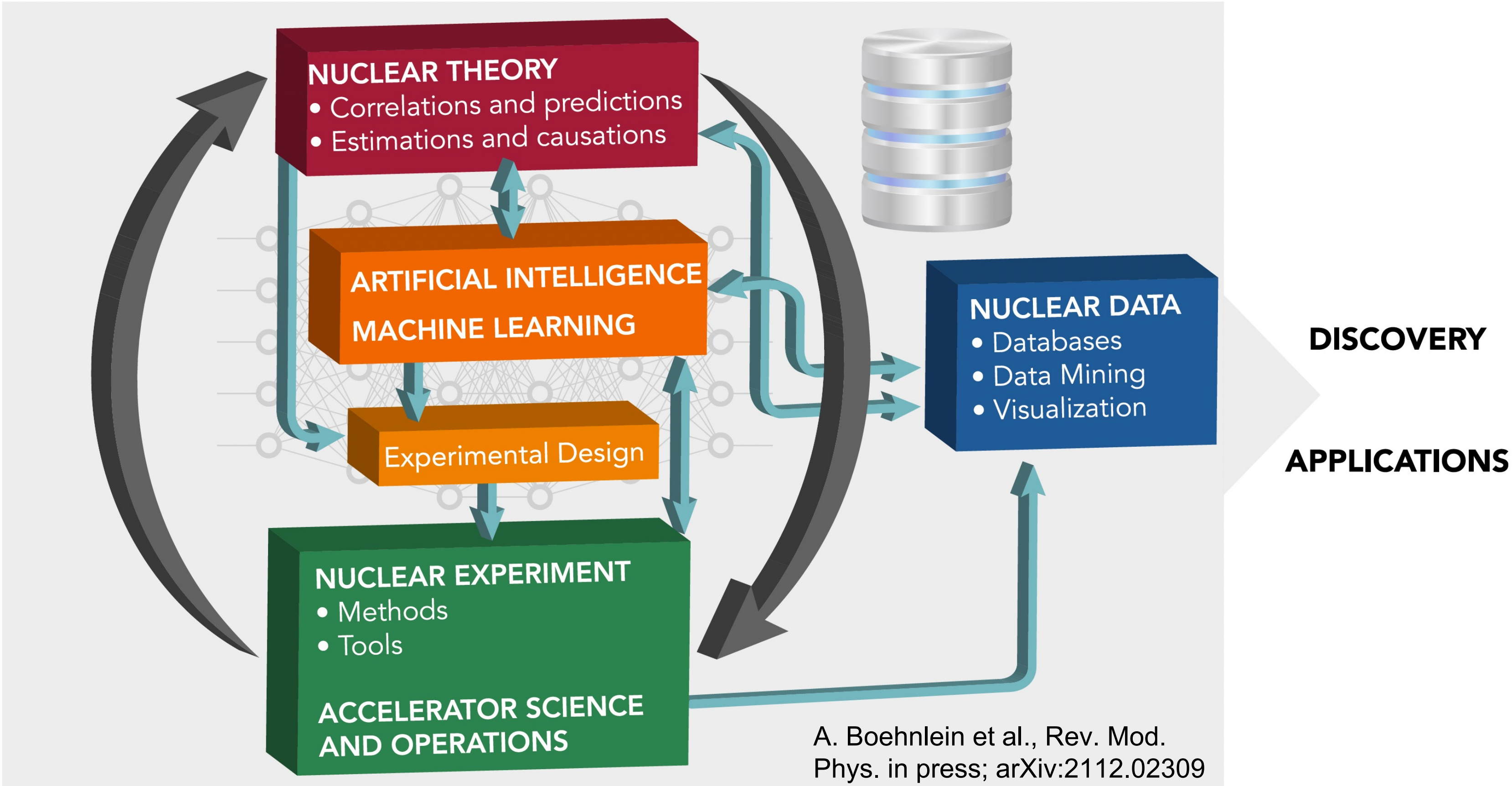

A. Boehnlein et al., Rev. Mod. Phys. in press; arXiv:2112.02309

Speeding-up the cycle of the scientific method

Uncertainty quantification (UQ) in low-energy nuclear theory

ML and statistical UQ tools can help us to speed up the scientific method cycle and hence facilitate discoveries

- Enabling fast emulation for big simulations
- Revealing the information content of measured observables with respect to theory
- Identifying crucial experimental data for better constraining theory
- Providing meaningful input to applications and planned measurements

ML and statistical UQ tools can help us to reveal the structure of our models

- Parameter estimation with heterogeneous/multi-scale datasets
- Model reduction

ML and statistical UQ tools can help us to provide predictive capability

- Uncertainty quantification essential
- Theoretical models are often applied to entirely new nuclear systems and conditions that are not accessible to experiment

Nuclear charge densities and charge radii

$$\rho_c(\boldsymbol{r}) = \frac{1}{(2\pi)^3} \int d^3q e^{-i\boldsymbol{q}\cdot\boldsymbol{r}} F_c(\boldsymbol{q})$$

nuclear charge density

nuclear charge form factor

$$F_c(\boldsymbol{q}) = \sum_{t\in\{p,n\}} \Big[G_{E,t}(\boldsymbol{q}) \left(1 - \tfrac{1}{2}\boldsymbol{q}^2\mathcal{D}\right) F_t(\boldsymbol{q}) - \mathcal{D}\left[2\mu_t G_{M,t}(\boldsymbol{q}) - G_{E,t}(\boldsymbol{q})\right] F_{\ell s,t}(\boldsymbol{q}) \Big].$$

$$\mathcal{D} = \frac{\hbar^2}{(2mc)^2}$$

$G_{E,t}$ and $G_{M,t}$ are the intrinsic nucleonic electromagnetic form factors

$$F_t(\boldsymbol{q}) = \int d^3r\, e^{i\boldsymbol{q}\cdot\boldsymbol{r}} \rho_t(\boldsymbol{r}),$$

$$F_{\ell s,t}(\boldsymbol{q}) = \int d^3r\, e^{i\boldsymbol{q}\cdot\boldsymbol{r}} \boldsymbol{\nabla}\cdot\boldsymbol{J}_t(\boldsymbol{r})$$

spin-orbit current

General expression. Valid for spherical and deformed nuclei. Slightly different expression in CDFT

Nuclear charge densities in spherical and deformed nuclei: Toward precise calculations of charge radii, P.G. Reinhard, WN, Phys. Rev. C 103, 054310 (2021)

$$\langle r_c^2\rangle = \langle r_{pp}^2\rangle + \langle r_p^2\rangle^{(\mathrm{intr})} + \frac{N}{Z}\langle r_n^2\rangle^{(\mathrm{intr})} + \langle r^2\rangle^{(\mathrm{rel})}$$

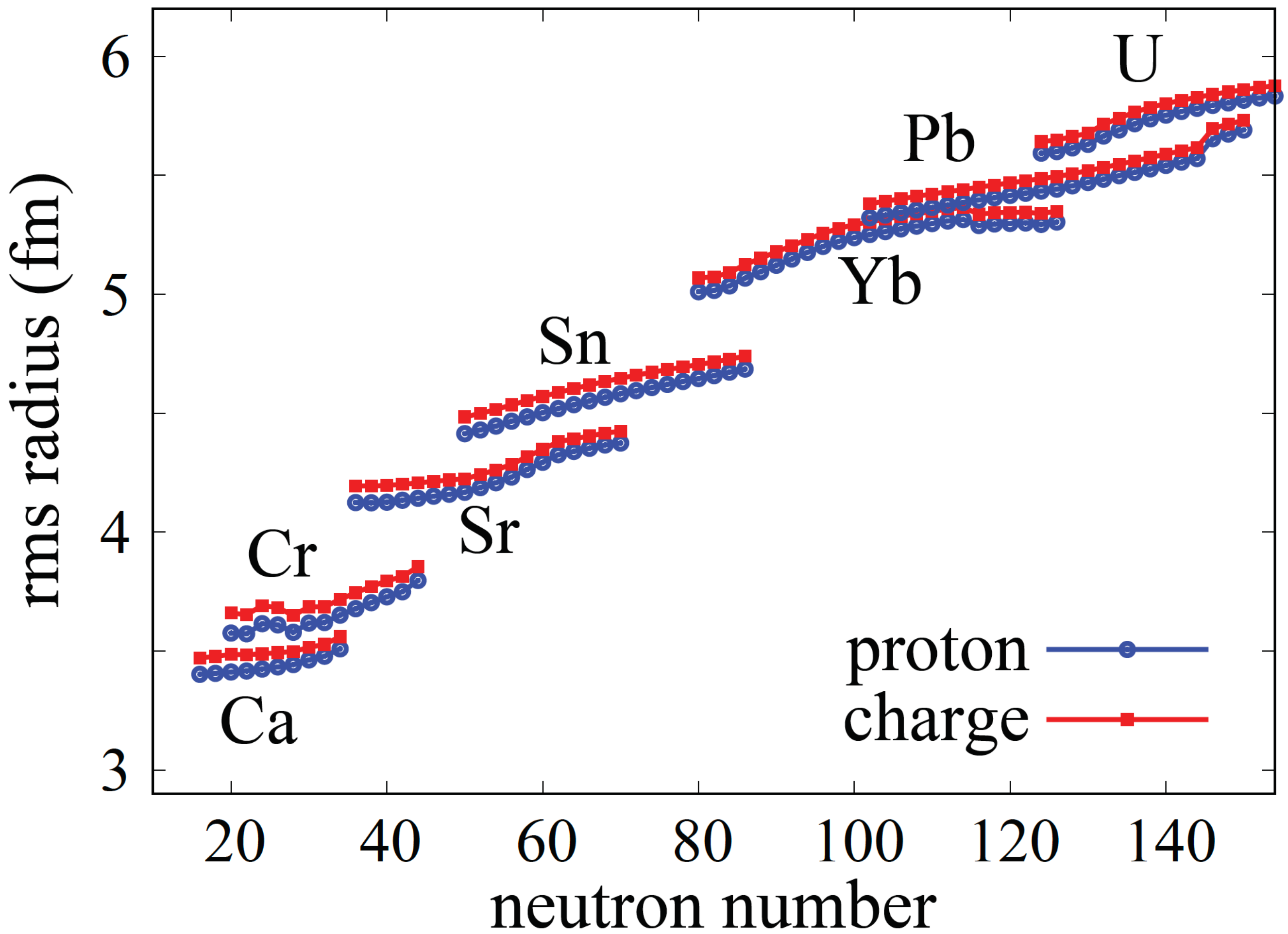

The relativistic correction must be included in precision calculations and studies of small local variations of charge radii such as the discontinuities across shell closures, which requires accuracy on charge radius prediction well below 0.01 fm.

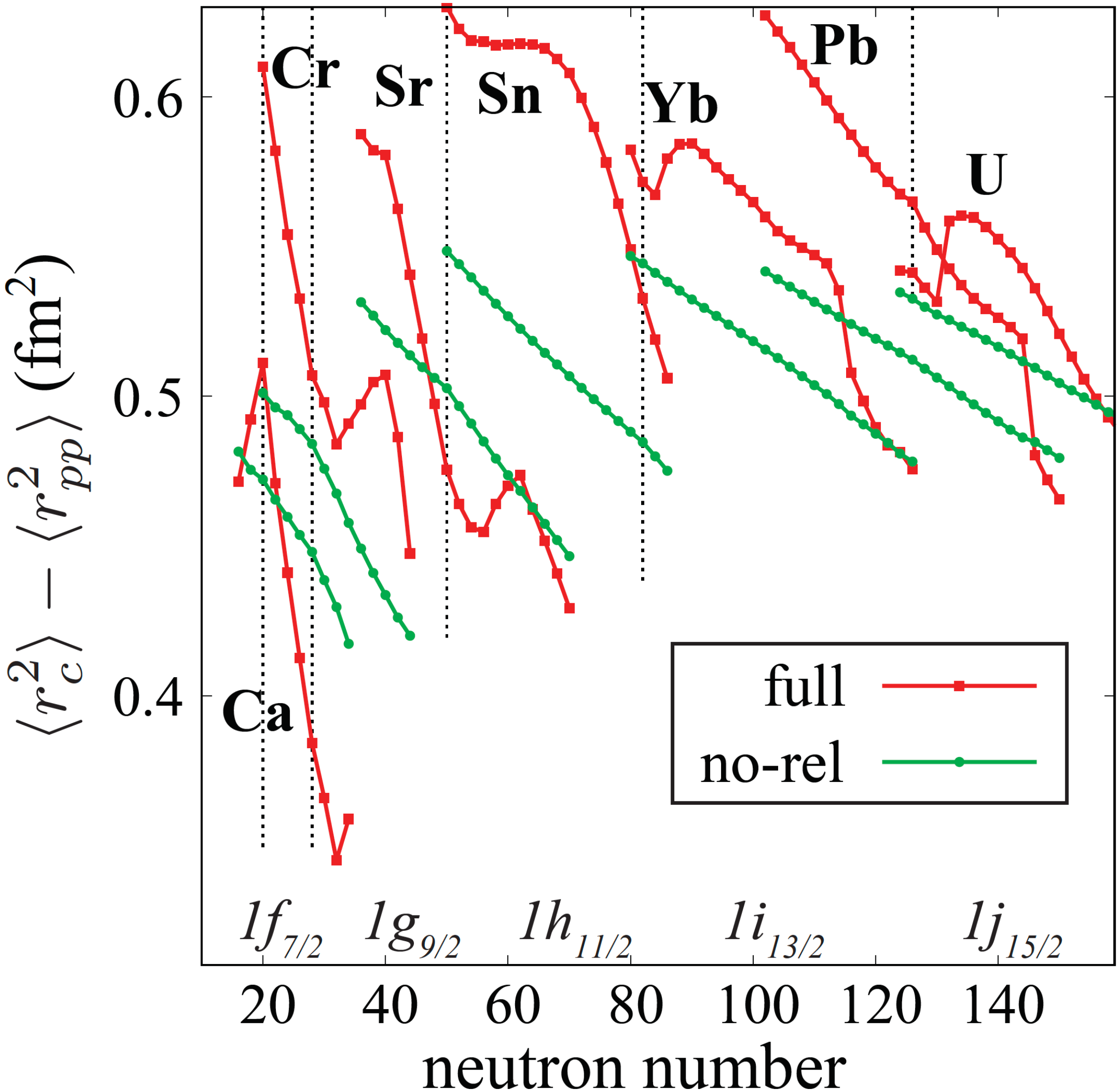

The spin- orbit contribution strongly fluctuates with N. In the regions corresponding to the gradual occupation of high-j unique- parity shells, the spin-orbit correction rapidly decreases due to the negative value of μ_n.

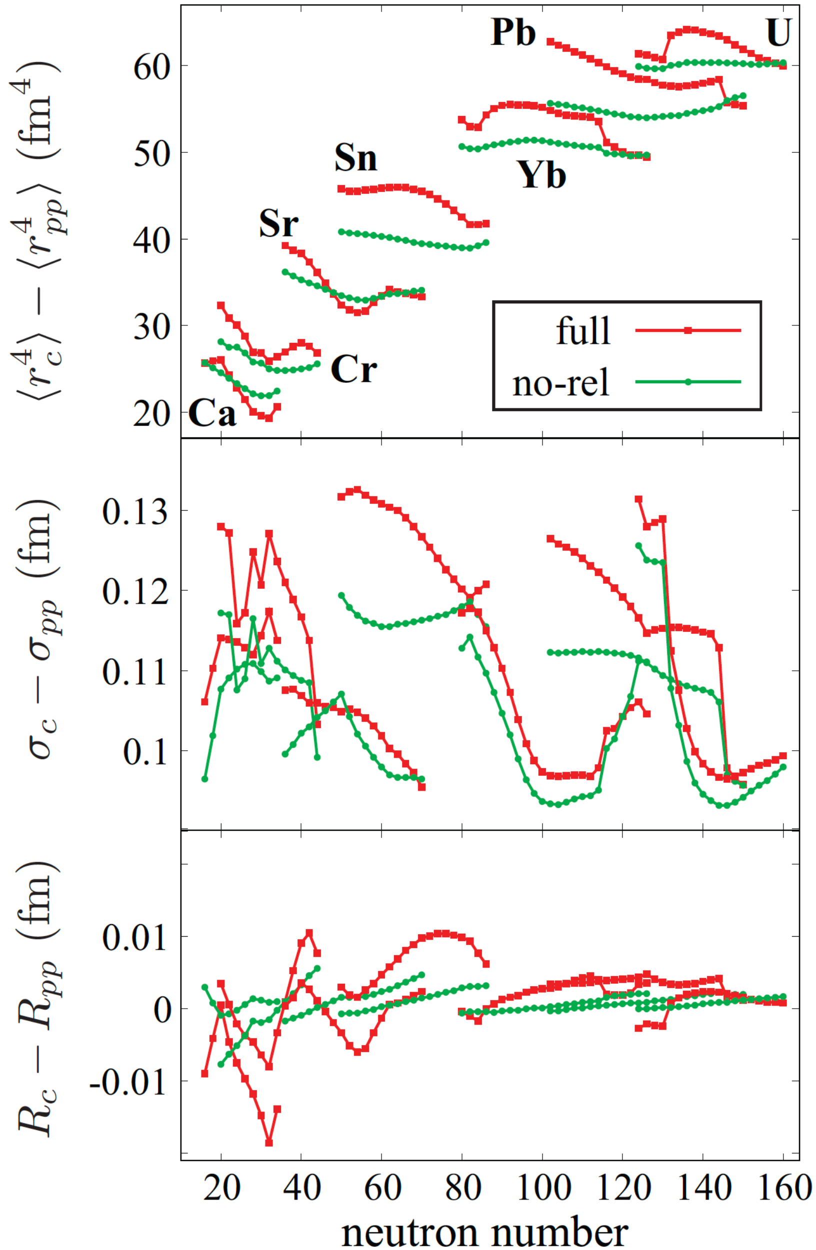

Beyond the charge radius: The information content of the fourth radial moment
P.-G. Reinhard, W.N., and R. F. Garcia Ruiz Phys. Rev. C 101, 021301(R) (2020)

Universal trend of charge radii of even-even Ca–Zn nuclei

M. Kortelainen et al., Phys. Rev. C 105, L021303 (2022).

Note the rapid increase of δr^2 above *N*=28: Nat. Phys.12, 594 (2016)

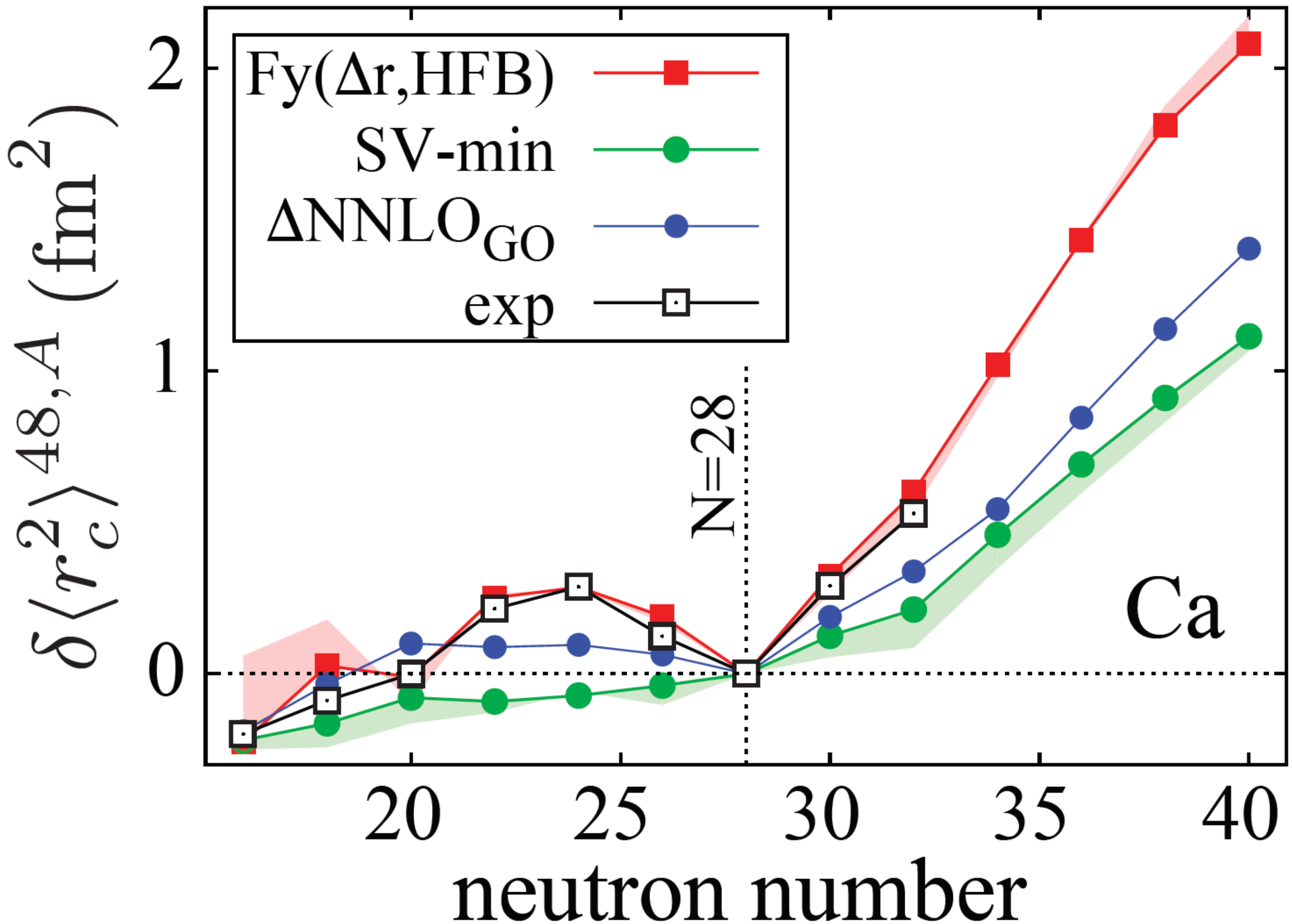

Amazing regularity for 28≤N≤40. Pseudo-SU(3) sd shell. Generalized seniority:

$$\delta\langle r_c^2\rangle^{A_\mathrm{m},A_\mathrm{m}+n} = an + bn^2$$

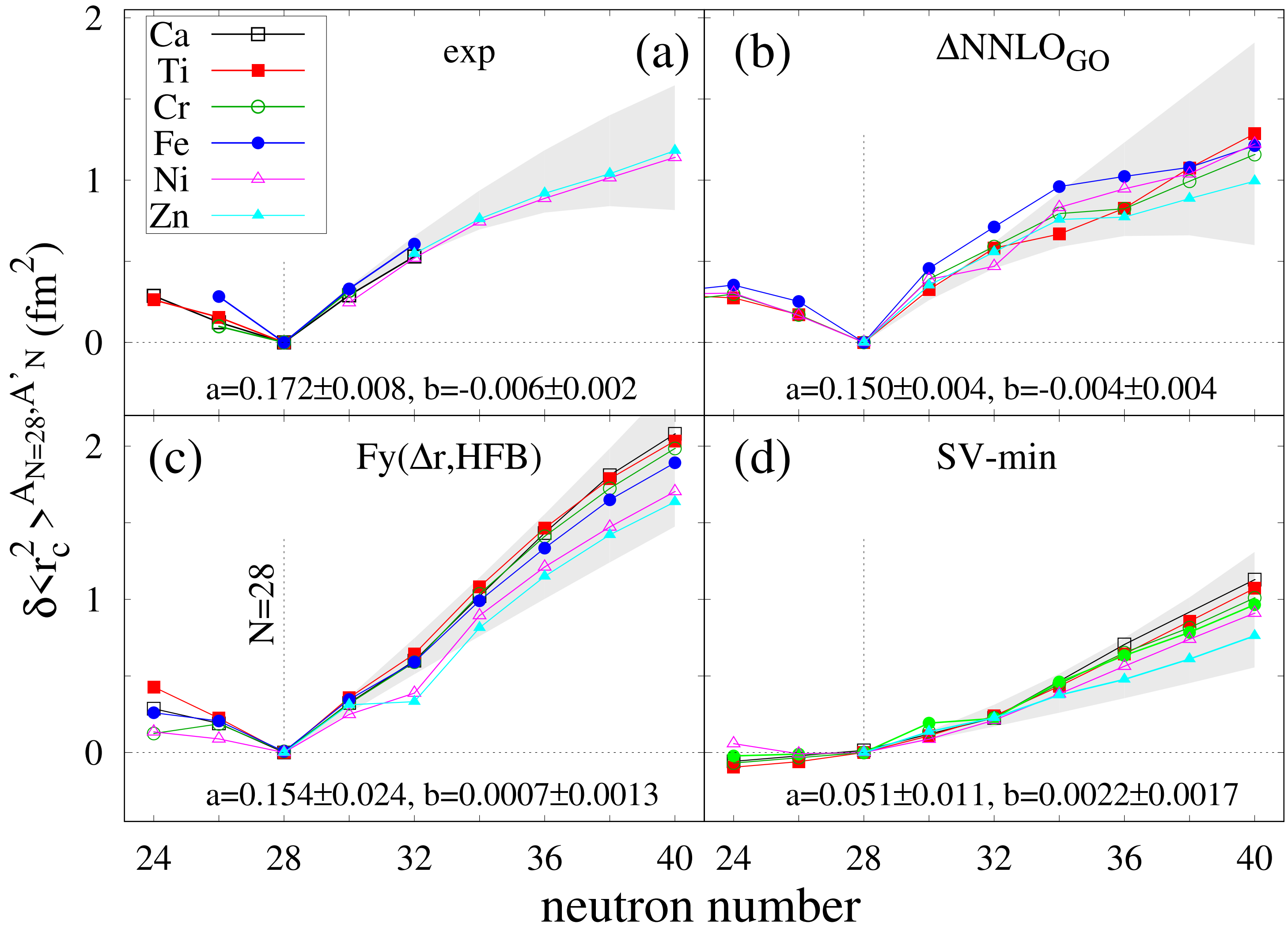

Odd–even staggering of charge radii of exotic copper isotopes

R.P. de Groote et al., Nat. Phys. 16, 620 (2020)

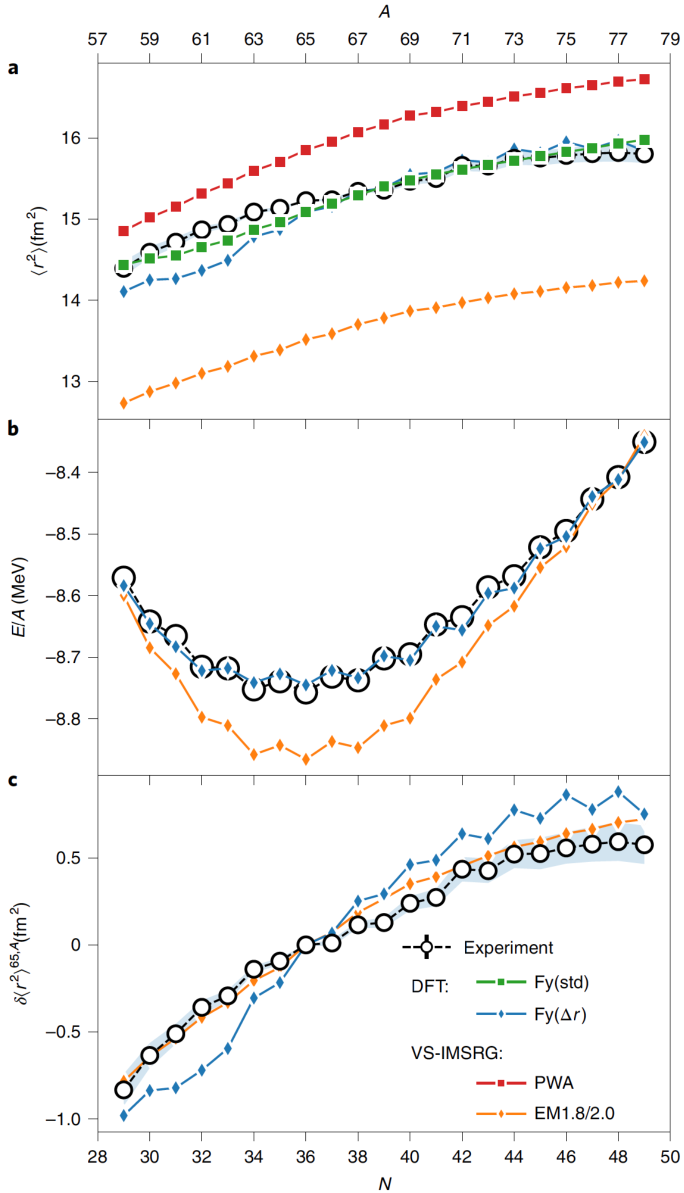

The interplay between the bulk nuclear properties (better captured by DFT) and local variations (better captured by VS-IMSRG calculations) was shown to be crucial in revealing the microscopic description of the OES effect in radii and binding energies

$$\Delta_r^{(3)} = \frac{1}{2}\left(r_{A+1} - 2r_A + r_{A-1}\right)$$

Odd–even staggering of charge radii of exotic copper isotopes

R.P. de Groote et al., Nat. Phys. 16, 620 (2020)

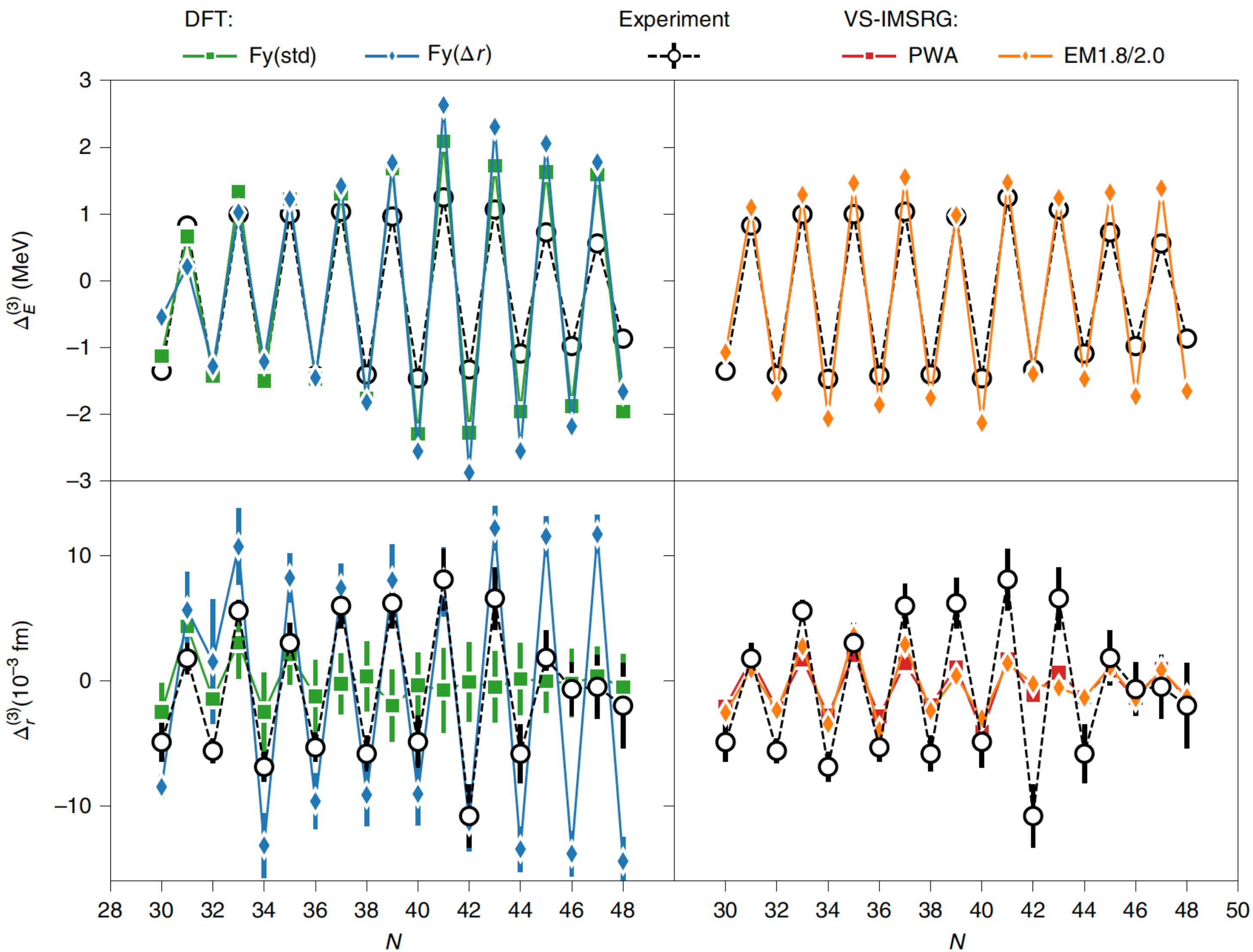

The OES effect in radii strongly impacted by the form of the pairing functional!

Information content of the differences in the charge radii of mirror nuclei

P.-G. Reinhard and WN. Phys. Rev. C 105, L021301 (2022)

$$\Delta R_{\rm ch}^{\rm mir}(^{A}X/Y) \equiv R_{\rm ch}(^{A}_{Z}X_{N}) - R_{\rm ch}(^{A}_{N}Y_{Z})$$

It has been suggested in Phys. Rev. Lett. 119, 122502 (2017) that a difference in the charge radii of mirror nuclei can serve as an isovector indicator that can be used to estimate the symmetry energy.

… but open-shell proton-rich mirror partners are superfluid and weakly bound!

To assess the correlation between mirror radii differences, we carried out statistical analysis.

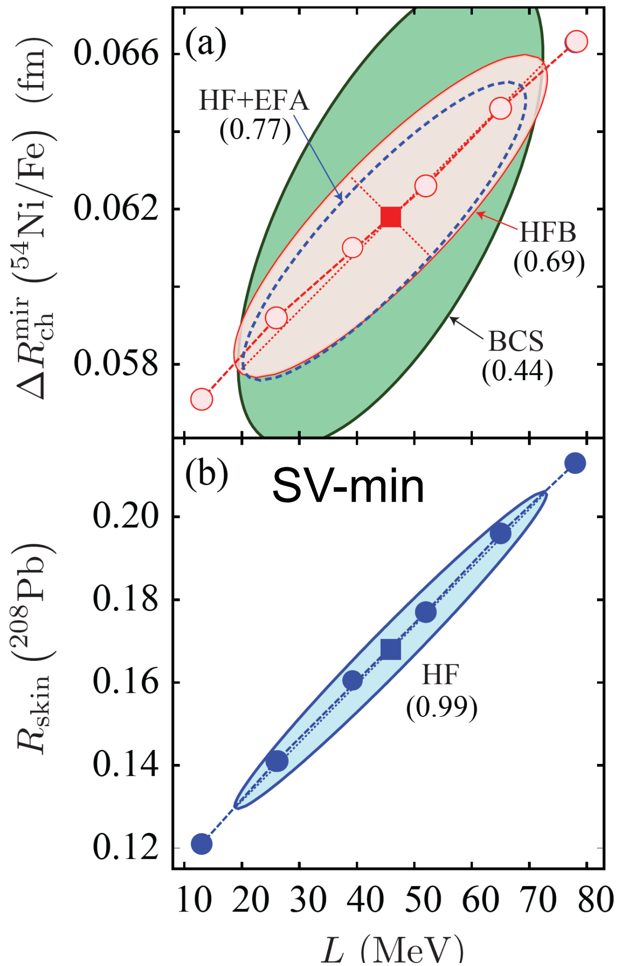

$$R_{x,y} = \frac{\mathrm{cov}(x,y)}{\sigma_x \sigma_y} \qquad \mathrm{CoD}(x,y) = R^2_{x,y}$$

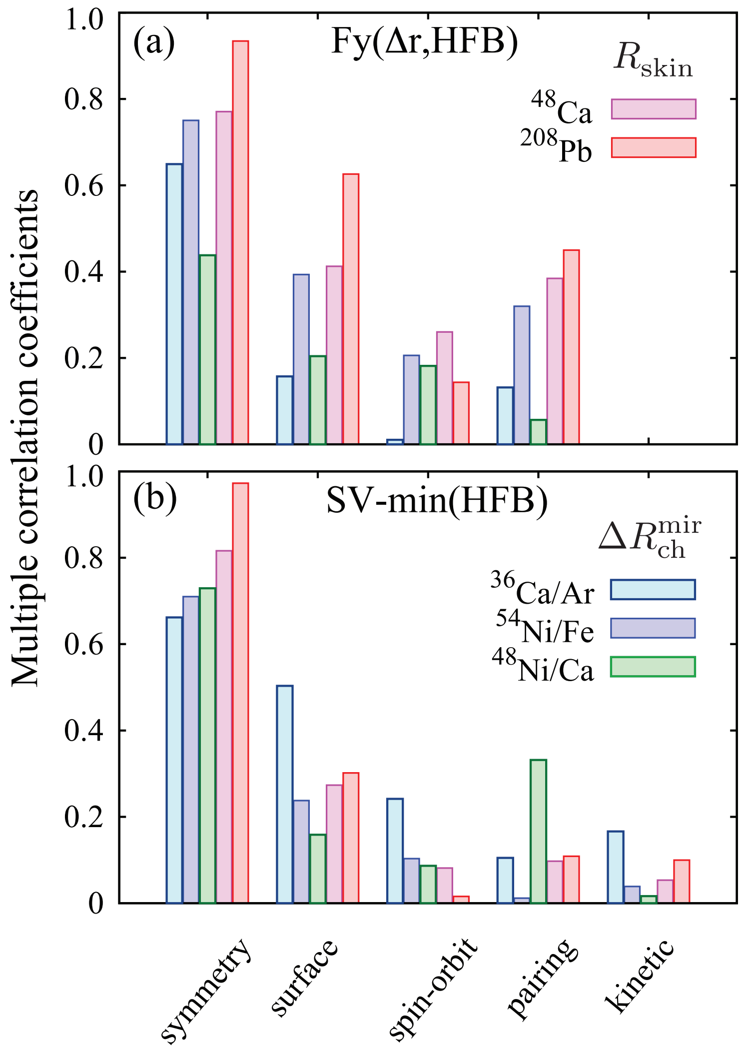

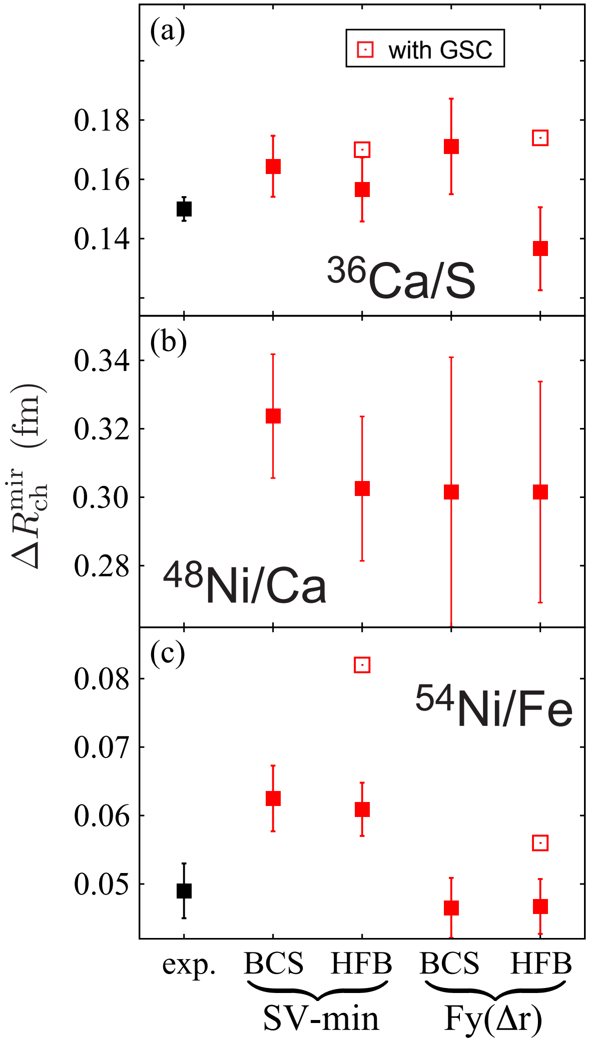

continuum effects important!

We conclude that the difference in charge radii between a mirror pair is *an inferior* isovector indicator compared to other observables, such at the neutron skin or electric dipole polarizability.

Statistical correlations of nuclear quadrupole deformations and charge radii, P.-G. Reinhard & WN, arXiv:2205.06139

$$R_{x,y} = \frac{\mathrm{cov}(x,y)}{\sigma_x \sigma_y}$$

bivariate correlation coefficient

$$\mathrm{CoD}(x,y) = R^2_{x,y}$$

coefficient of determination

variance of difference: $$\sigma^2_{x-y} = \sigma^2_x + \sigma^2_y - 2R_{x,y}\sigma_x\sigma_y.$$

$$R_{x,y} \approx 1 \quad \longrightarrow \quad \sigma_{x-y} \approx |\sigma_x - \sigma_y|$$

Are variances of differences of smoothly varying observables small?

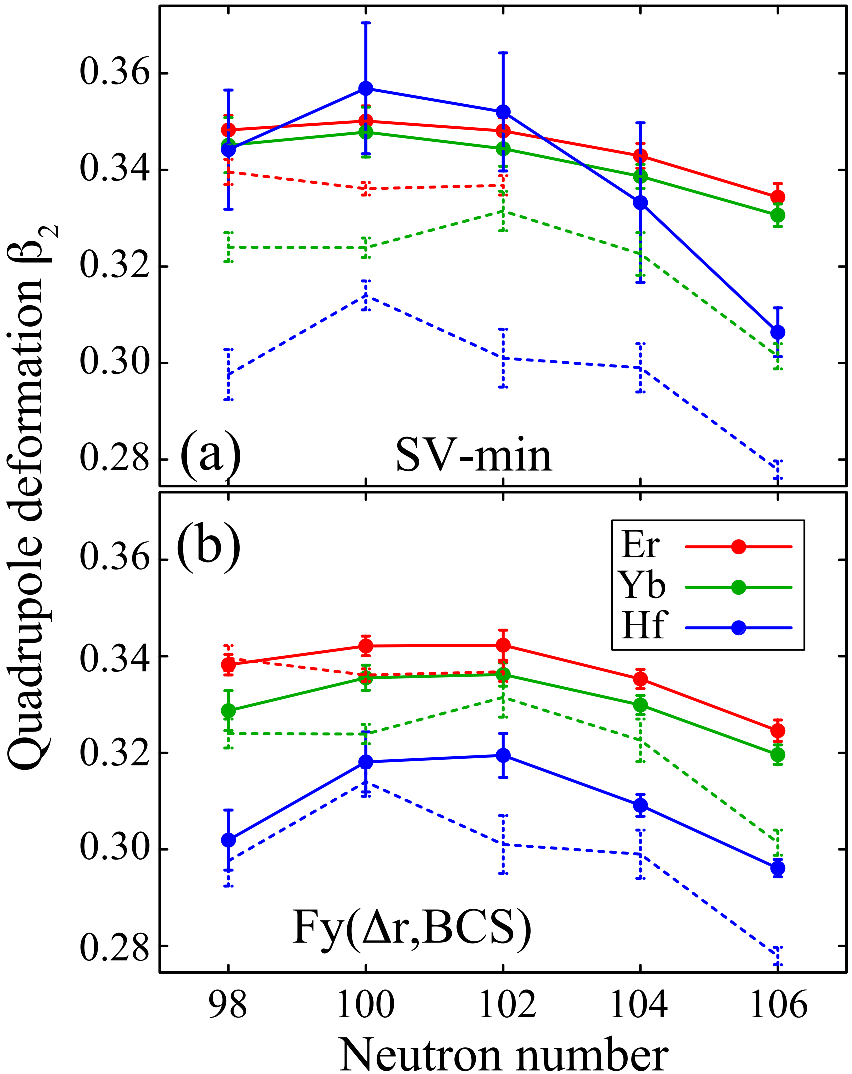

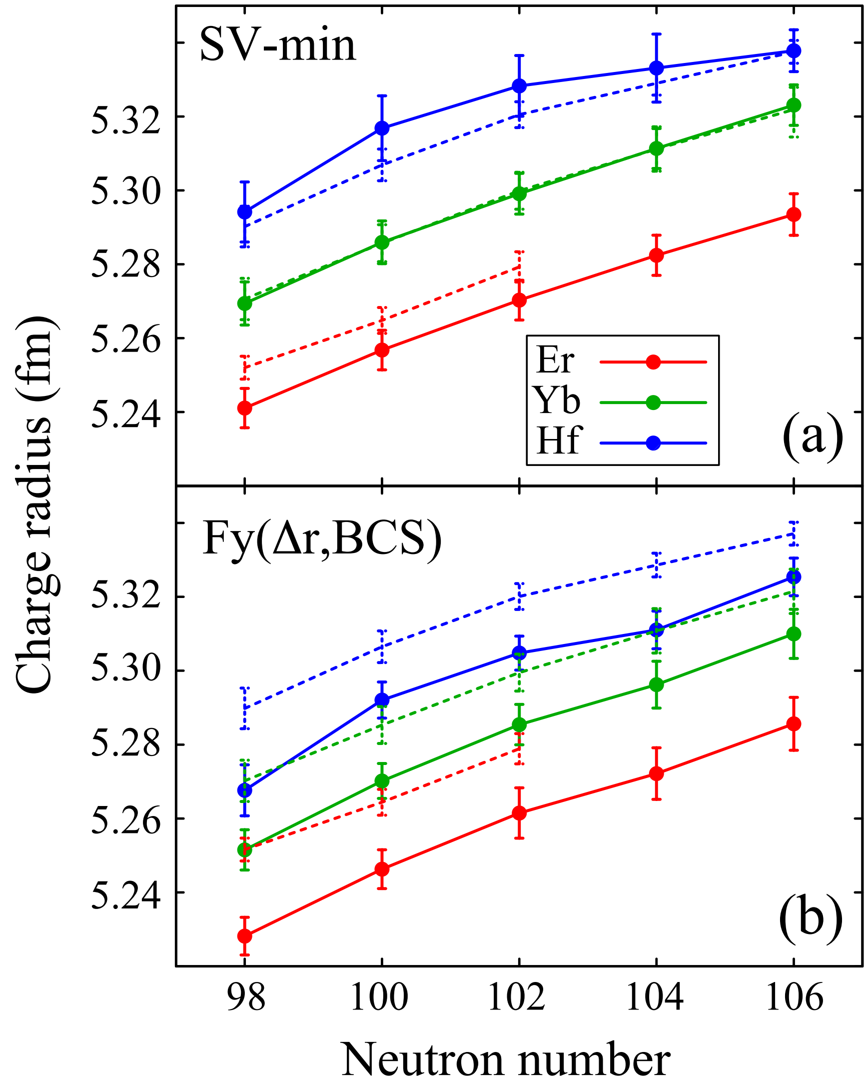

Quadrupole deformations and charge radii vary smoothly!

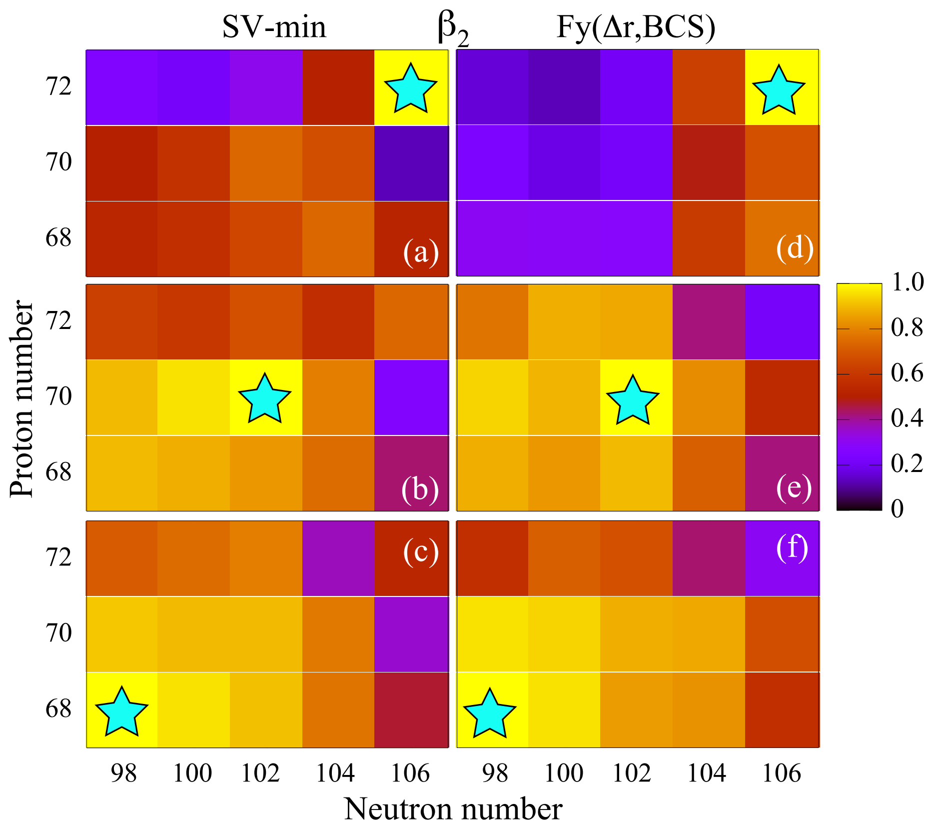

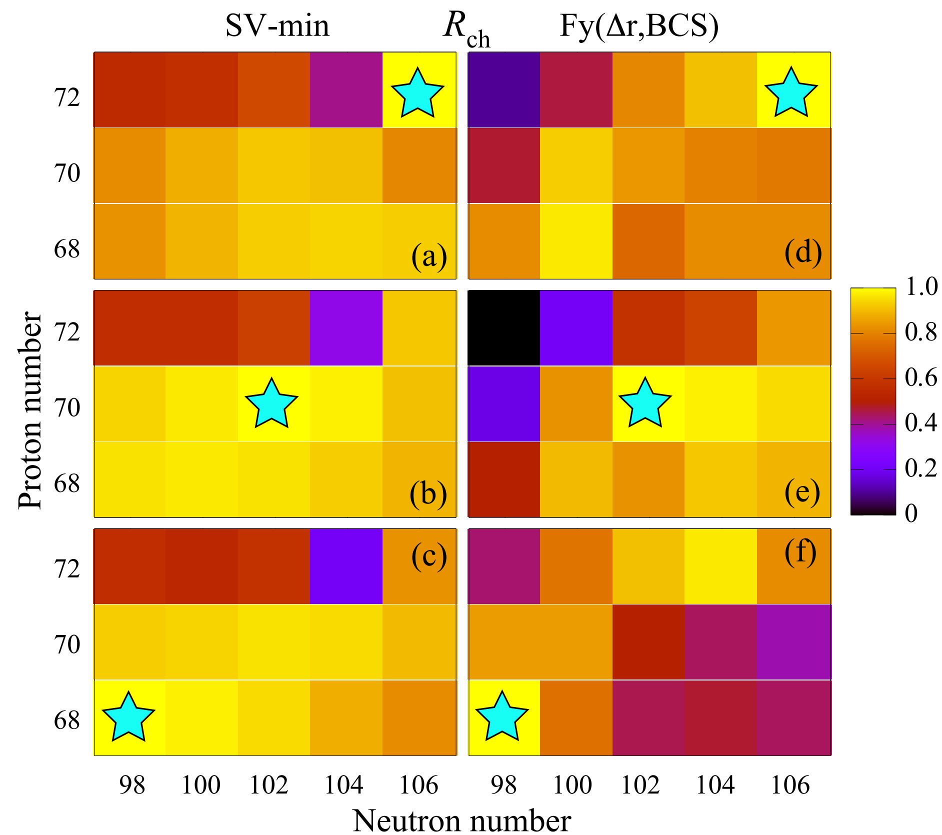

The calculated CoD diagrams show patterns that are surprisingly localized as compared to the smooth trends of observables.

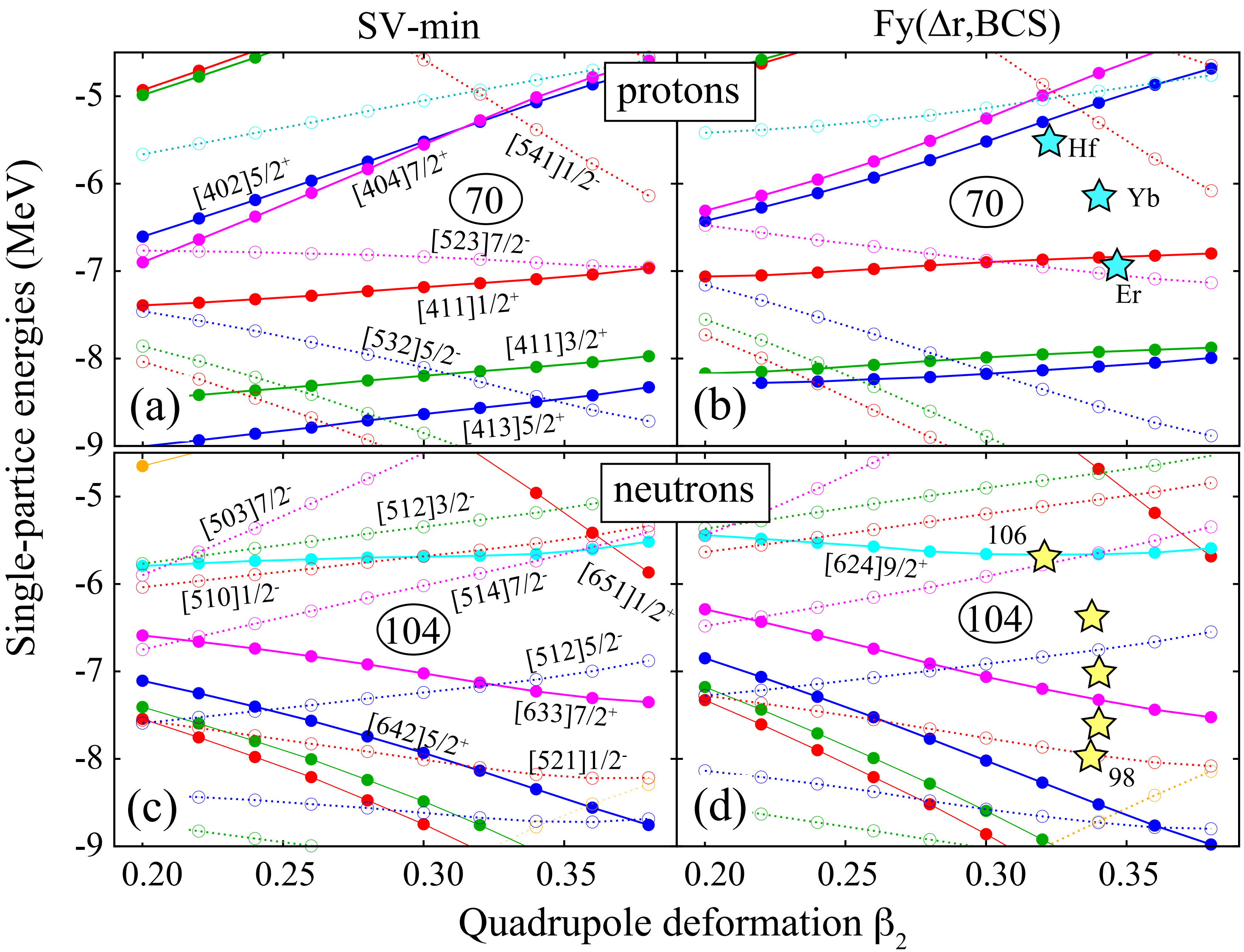

The local variations of CoDs reflect the underlying deformed shell structure and changes of single-particle configurations

Evidence of two-source King plot nonlinearity in spectroscopic search for new boson

J. Hur et al., Phys. Rev. Lett. 128, 163201 (2022)

It has been suggested that atomic systems can be used to search for unknown particles which are dark-matter candidates. The new forces mediated by these particles may slightly disturb the structure of atoms by changing the color of light that the atoms resonate with. To this end, precise measurement of the resonating electromagnetic transitions in the stable even-even ytterbium atoms has been carried out by the MIT group. The measurement observed the unknown patterns that are inconsistent with standard expectations.

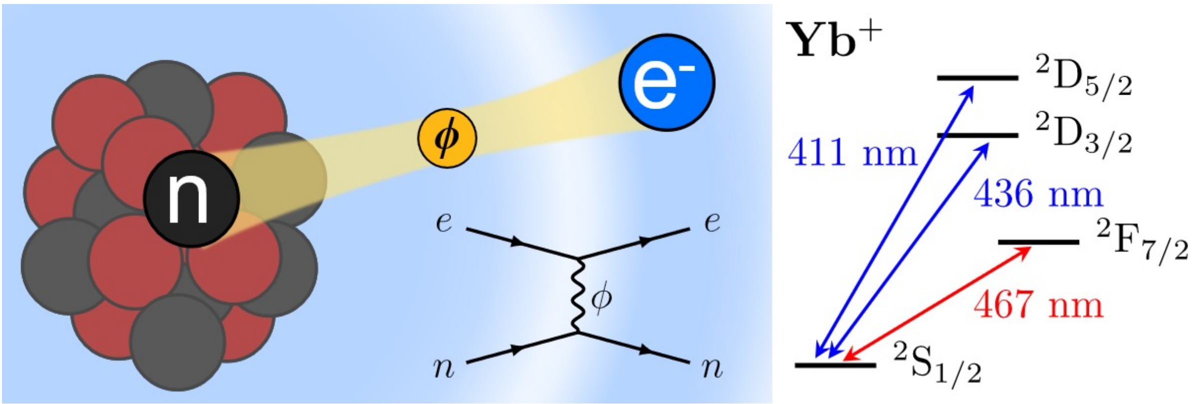

$$\nu_\gamma^{AA'} = F_\gamma \delta\langle r^2\rangle^{AA'} + K_\gamma \mu^{AA'} + G_\gamma^{(4)} \delta\langle r^4\rangle^{AA'} + G_\gamma^{(2)} [\delta\langle r^2\rangle^2]^{AA'} + \upsilon_{ne} D_\gamma a^{AA'} + \cdots$$

The careful analysis, involving advanced atomic theory and nuclear theory, combined with other recent results, suggests that the observed deviations *primarily originate from nuclear effects* related to charge radii and shape deformations.

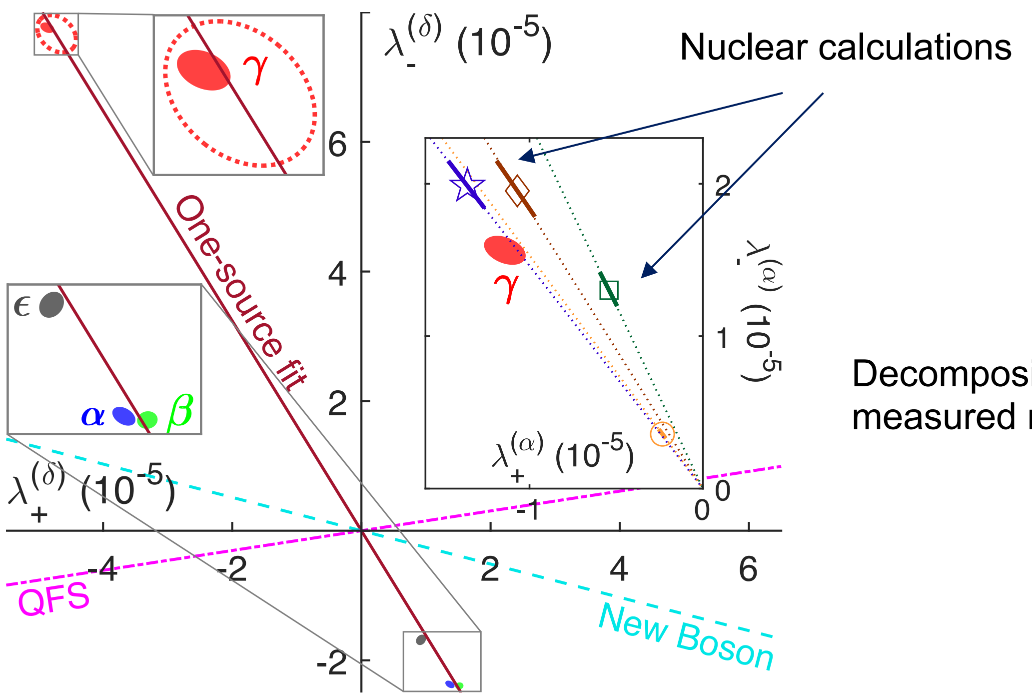

Decomposition of the measured nonlinearity

PREX-2 and CREX assessment

$$A_{\rm PV}(Q^2) = \frac{d\sigma_R/d\Omega - d\sigma_L/d\Omega}{d\sigma_R/d\Omega + d\sigma_L/d\Omega}$$

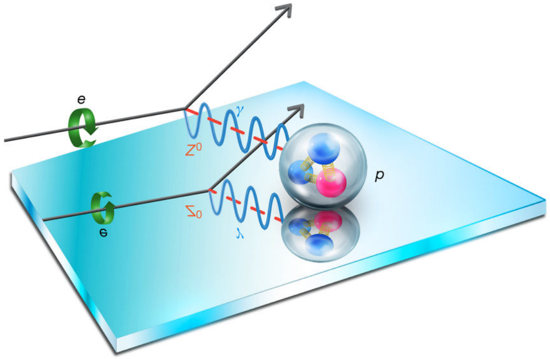

Adhikari et al., Phys. Rev. Lett. 126, 172502 (2021) measured $A_{\rm PV}$ for ^{208}Pb at a single kinematic condition (transferred momentum q=0.3978/fm): $A_{\rm PV}$ =550 ±16 (stat) ±8 (syst)

Adhikari et al., arXiv:2205.11593 (2022) measured $A_{\rm PV}$ for ^{48}Ca at a single kinematic condition (transferred momentum q=0.8733/fm): $A_{\rm PV}$ =2668 ±106 (stat) ±40 (syst)

The new experimental information provided by PREX-2 and CREX is the $A_{\rm PV}$ measured at a specific kinematic condition. Other nuclear quantities of interest reported, such as the neutral weak form factor, neutron skin thickness, interior weak density, interior baryon density, and symmetry energy parameters, become accessible only via theoretical models.

$$A_{\rm PV} \xrightarrow{\mathcal{M}} F_W(q) \xrightarrow{\mathcal{M}} R_{\rm skin}, J, L$$

Theoretically:

$$A_{\rm PV}(Q^2) \approx \frac{G_F Q^2 |Q^{(W)}_{N,Z}|}{4\sqrt{2}\,\pi\alpha Z}\,\frac{F_W(q)}{F_C(q)}$$

Coulomb distortions must be considered…

$$F_C(q) = \frac{e^{a_{\rm cm} q^2}}{Z}\sum_{t=p,n}\left[G_{E,t}(q)F_t(q)+G_{M,t}(q)F_t^{(ls)}(q)\right]$$

$$F_W(q) = \frac{e^{a_{\rm cm} q^2}}{ZQ_p^{(W)}+NQ_n^{(W)}}\sum_{t=p,n}\left[G_{E,t}^{(W)}(q)F_t(q)+G_{M,t}^{(W)}(q)F_t^{(ls)}(q)\right]$$

G_E and G_M are the intrinsic proton and neutron electromagnetic/weak form factors

$$Q_n^{(W)} = -0.9888 \pm 0.0011 \qquad Q_p^{(W)} = 0.0713 \pm 0.0001$$

Information content of the parity-violating asymmetry in ^{208}Pb and ^{48}Ca

P.-G. Reinhard, X. Roca-Maza, WN, Phys. Rev. Lett. 127, 232501 (2021)
and arXiv: 2206.03134 (2022)

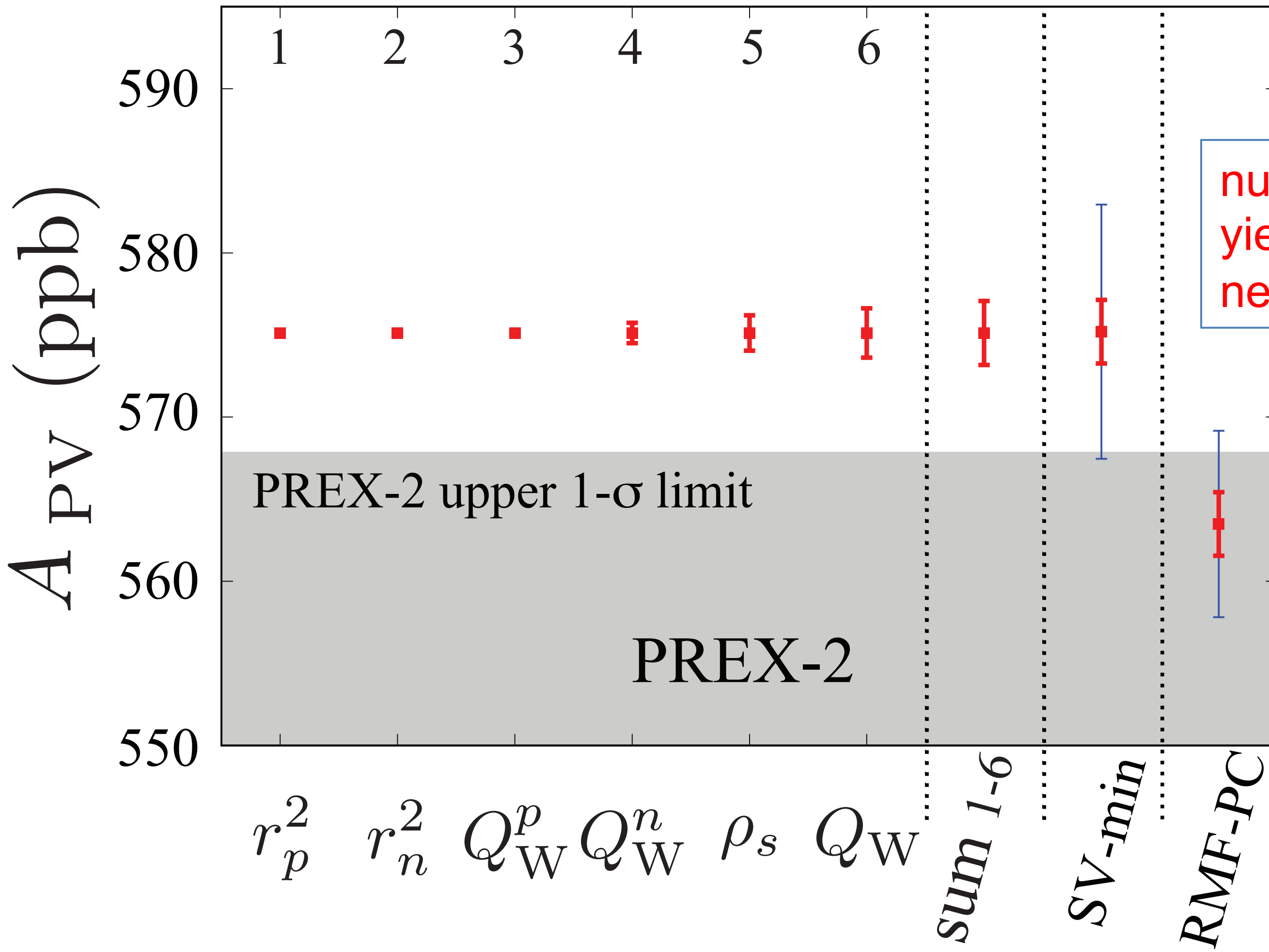

nuclear DFT models yield proton and neutron densities

Theoretical uncertainty on A_{PV} is close to systematic error of PREX-2

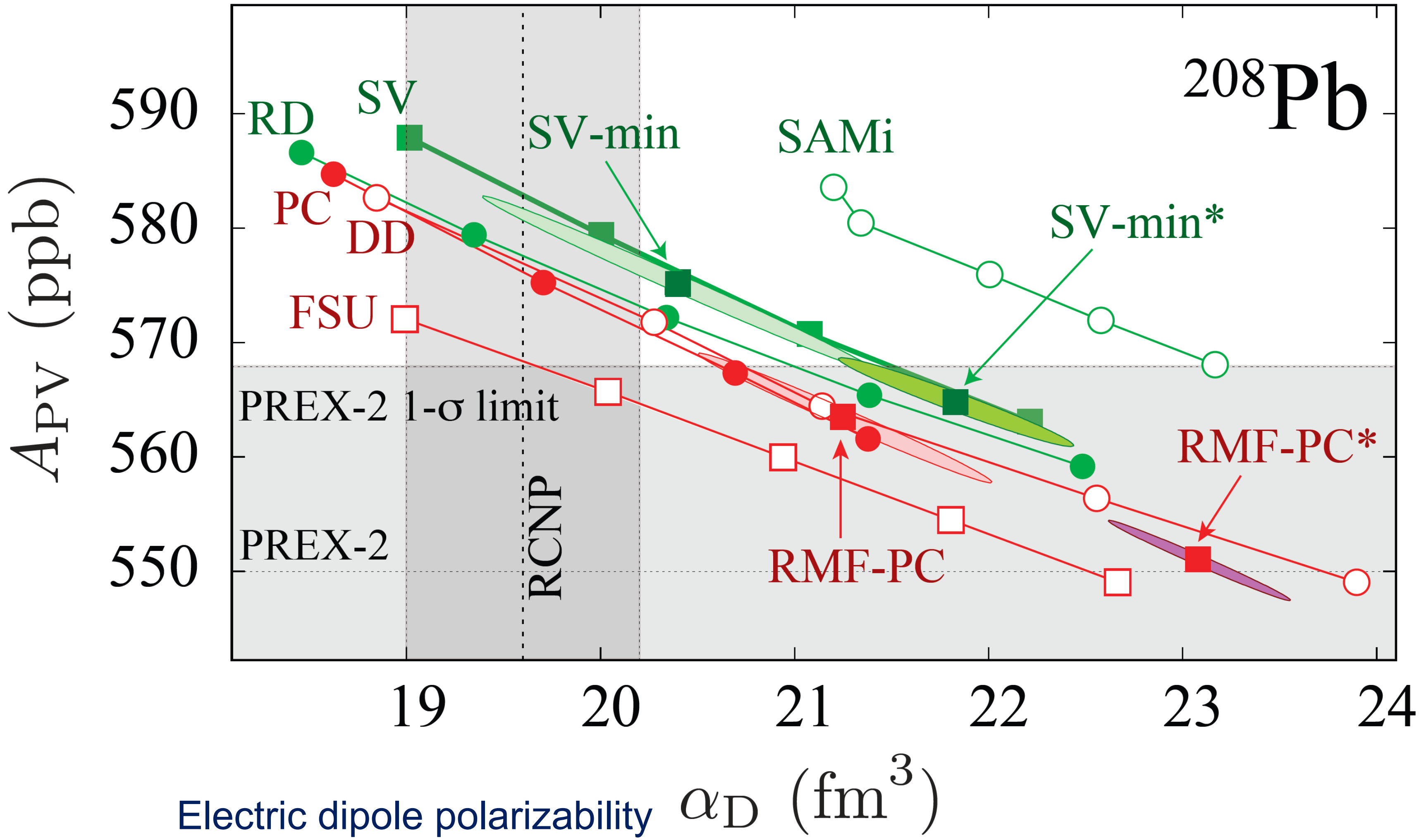

Electric dipole polarizability

- SV-min* and RMF-PC* we constrained to experimental values of A_{PV} and α_D
- There is a clear tension between A_{PV} and α_D

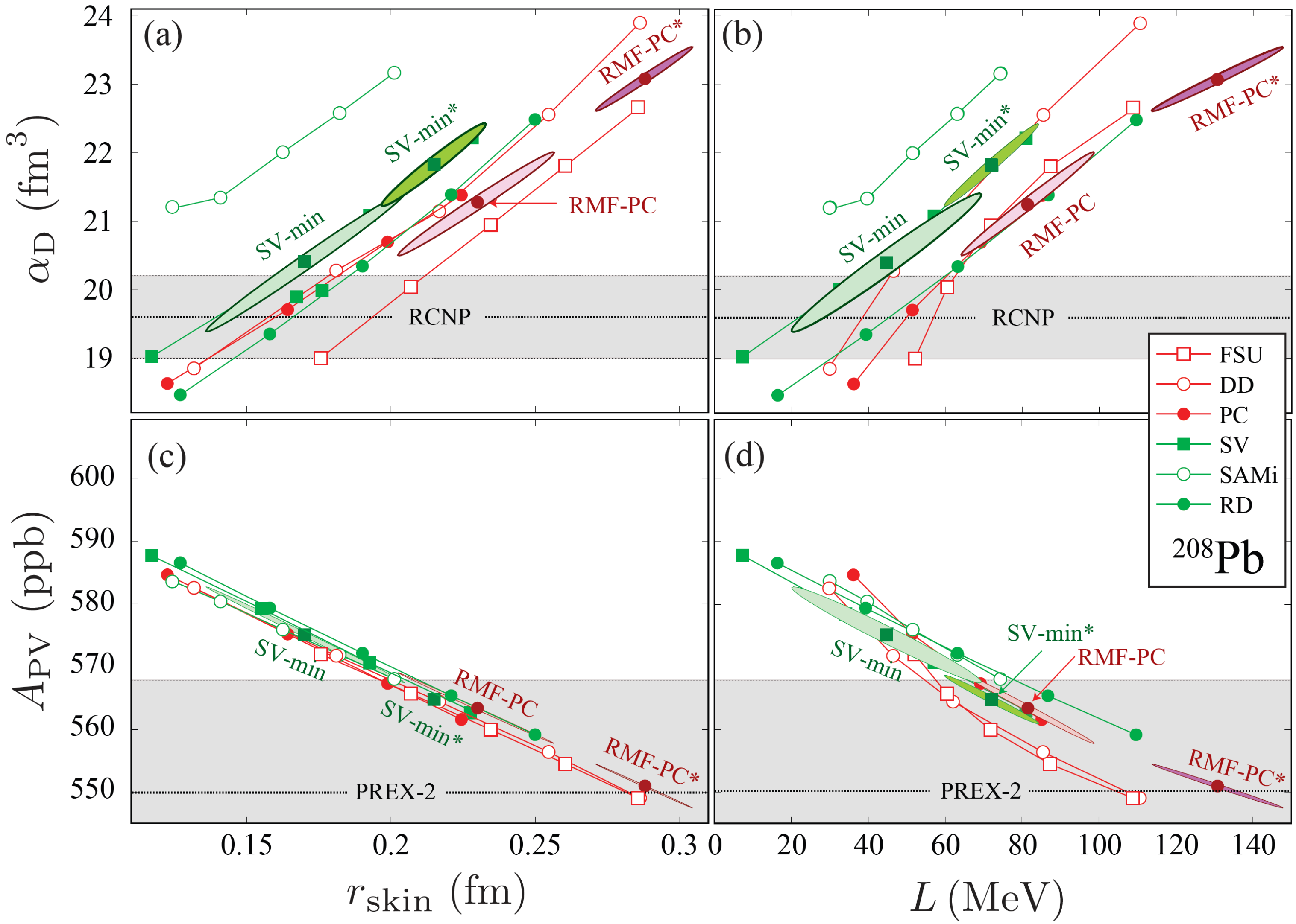

Based on our calibrated results, we predict a neutron skin thickness in ^{208}Pb r_{skin} = 0.19±0.02 fm and the symmetry-energy slope L = 54 ± 8 MeV. These values are consistent with other estimates based on astrophysical data and are significantly lower than those reported by Reed et al. in Phys. Rev. Lett. 126, 172503 (2021).

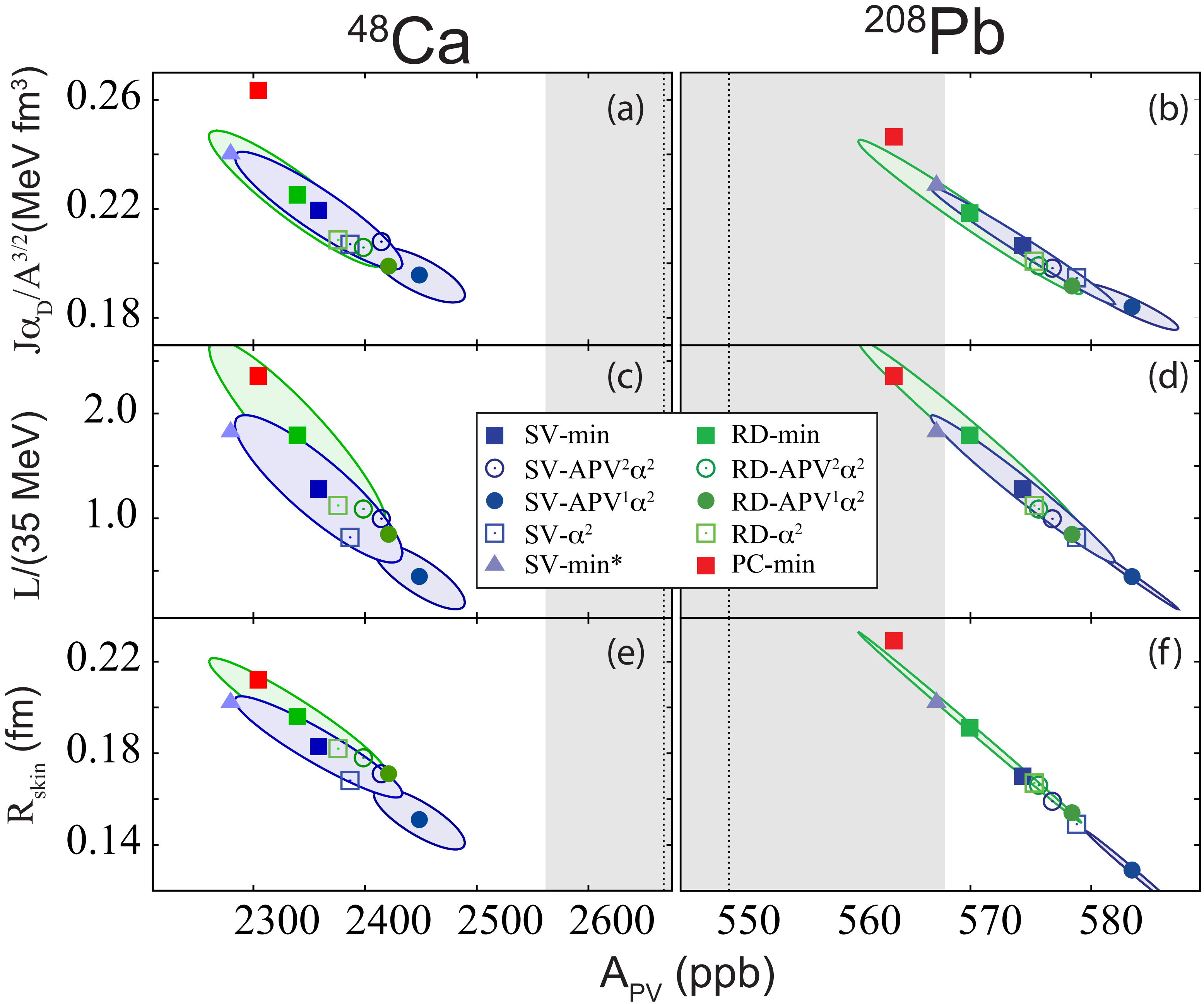

48Ca
208Pb
(a)
(b)
(c)
(d)
(e)
(f)
0.26
0.22
0.18
2.0
1.0
0.22
0.18
0.14
2300
2400
2500
2600
550
560
570
580
JαD/A3/2(MeV fm3)
L/(35 MeV)
Rskin (fm)
APV (ppb)
SV-min
SV-APV2α2
SV-APV1α2
SV-α2
SV-min*
RD-min
RD-APV2α2
RD-APV1α2
RD-α2
PC-min

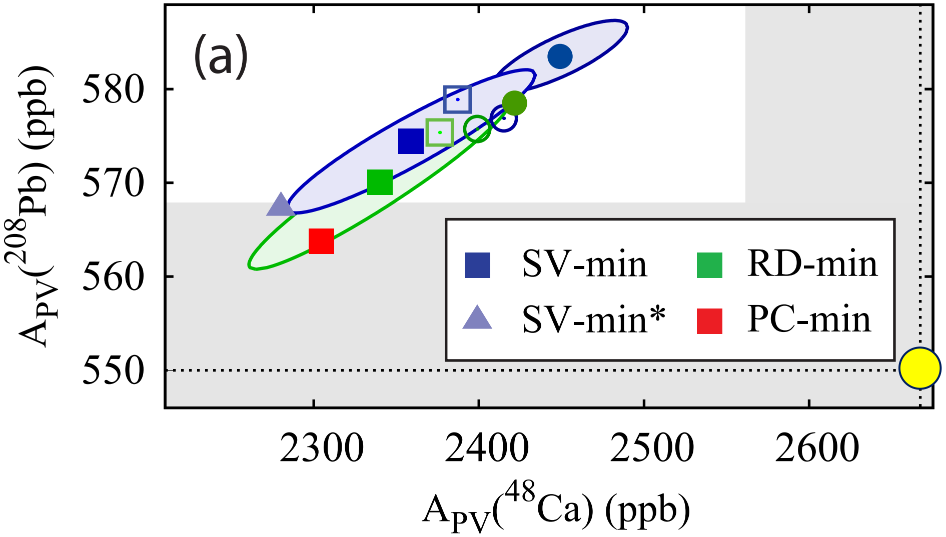

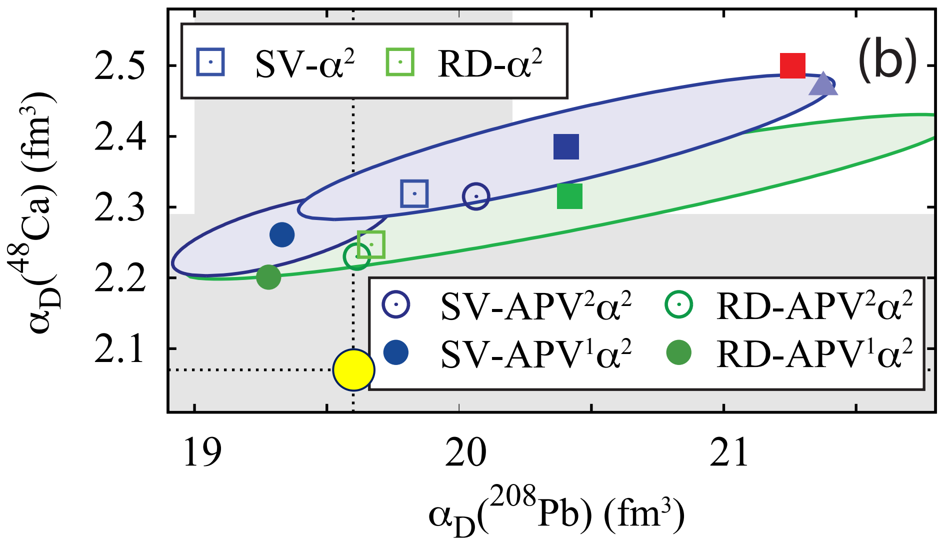

A tension between the A_{pv} data and global nuclear EDFs

or

The values of CREX and PREX-2 are not mutually compatible considering the current theory

The significant uncertainties of PREX-2 and CREX values of A_{pv} make it difficult to use this observable as a meaningful constraint on the isovector sector of current EDFs.

Until the tension between theory and experiment, or between the two measurements, is resolved, one should exercise extreme caution when interpreting the A_{pv} values in the context of neutron skins or nuclear symmetry energy.

Conclusions

Precise measurements of electroweak effects offer sensitivity to explore basic properties of the atomic nucleus and study fundamental symmetries. The new-generation data on electroweak form factors and moments impose higher precision requirements on a theoretical description.

Precise calculations of nuclear charge densities are needed to describe precise experimental data. Precise calculations are also important when developing high-quality nuclear energy density functionals optimized using heterogeneous datasets involving absolute charge radii, differential charge radii, and charge form factor properties deduced from electron scattering data.

BACKUP